Available online at www.sciencedirect.com
ScienceDirect
Biochimica et Biophysica Acta 1774 (2007) 249–257
Biochimica et Biophysica Acta
BBA
www.elsevier.com/locate/bbapap

How does dextran sulfate prevent heat induced aggregation of protein?: The mechanism and its limitation as aggregation inhibitor

Kwanghun Chung, Juhan Kim, Byung-Kwan Cho, Byoung-Joon Ko, Bum-Yeol Hwang, Byung-Gee Kim *

School of Chemical and Biological Engineering, Seoul National University, Seoul 151-742, Korea
Institute of Molecular Biology and Genetics, Seoul National University, Seoul 151-742, Korea

Received 11 July 2006; received in revised form 2 November 2006; accepted 30 November 2006
Available online 6 December 2006

Abstract

The effect of dextran sulfate on protein aggregation was investigated to provide the clues of its biochemical mechanism. The interaction between dextran sulfate and BSA varied with the pH values of the solution, which led to the different extent of aggregation prevention by dextran sulfate. Light scattering data with thermal scan showed that dextran sulfate suppressed BSA aggregation at pH 5.1 and pH 6.2, while it had no effect at pH 7.5. Isothermal titration calorimetric analysis suggested that the pH dependency of the role of dextran sulfate on BSA aggregation would be related to the difference in the mode of BSA–dextran sulfate complex formation. Isothermal titration calorimetric analysis at pH 6.2 indicated that dextran sulfate did not bind to native BSA at this pH, but interacted with partially unfolded BSA. While stabilizing native form of protein by the complex formation has been suggested as the suitable mechanism of preventing aggregation, our observation of conformational changes by circular dichroism spectroscopy showed that strong electrostatic interaction between dextran sulfate and BSA rather facilitated the denaturation of BSA. Combining the data from isothermal titration calorimetry, circular dichroism, and dynamic light scattering, we found that the complex formation of the intermediate state of denatured BSA with dextran sulfate is a prerequisite to suppress the aggregation by preventing further oligomerization/aggregation process of denatured protein.

Keywords: Protein aggregation; Dextran sulfate; Demixing; Protein denaturation

1. Introduction

The aggregation of proteins is involved in a wide variety of biomedical and biological phenomena including abnormal disorders such as neurodegenerative diseases and Alzheimer's disease [1]. In the molecular mechanism of protein aggregation, several studies revealed that proteoglycans (PGs) and glycoaminoglycans (GAGs) play a pivotal role in the formation of protein aggregates [4,5]. With regards to neurodegenerative diseases, there are numerous evidences that GAGs are involved in the formation of the amyloid deposits. In relation to Alzheimer's disease, the sulfated GAG–tau interaction was suggested to be the central event in the development of neuropathology [1–5]. Fibrillization of purified recombinant α-synuclein was also inefficient in vitro but could be enhanced by the addition of GAGs [5–7].

To shed new light on these phenomena, a number of studies have focused on the mechanism of GAGs–protein interaction. One important example is the formation of a β-sheet structure of the cognate proteins by GAGs. The proteins and polypeptides forming the β-structures by heparin appear to have the heparin binding sequences consisted of alternating basic and nonbasic amino acid residues [8]. In the formation of nucleation seeds, formation of the β-sheet structure would cause the alternating basic side chains to point to the same direction perpendicular to the plain of the sheet [9–11]. GAGs, as a scaffold, bound to the basic side chains and enhanced the structural features favoring the β-sheet conformation and accelerated the formation of nucleation seeds [12,13]. In the latter stages of the amyloid pathway, GAGs also enhanced the lateral aggregation of small fibrils to confer insolubility and to

* Corresponding author. Mailing address: School of Chemical and Biological Engineering, Seoul National University, Seoul 151-742, Korea. Tel.: +82 2 880 6774; fax: +82 2 883 6020.
E-mail address: byungkim@snu.ac.kr (B.-G. Kim).

1570-9639/$ - see front matter © 2006 Elsevier B.V. All rights reserved.
doi:10.1016/j.bbapap.2006.11.015

protect them from proteolysis. In this example, GAGs played a role as an enhancer of propagation, possibly by serving as an anchor for fibril organization or by stabilizing the tertiary structure of the fibril [12].

In contrast to the aggregation facilitating effect of GAGs on pathological proteins, many previous studies have also revealed that GAGs can prevent protein aggregation [14–17,38]. However, the biochemical mechanism of the sulfated polysaccharides for preventing heat induced protein aggregation remains relatively unclear and controversial. Very low concentrations of heparin could effectively suppress the aggregation of Antithrombin III [14]. It was suggested that the heparin stabilizes the protein by holding it in a conformationally altered but native state, presumably reducing the amplitude of dynamic fluctuations which could produce momentary exposure of hydrophobic moieties to the aqueous solvent, and as a result, aggregation is suppressed [14]. Heat-denatured RNaseA aggregation was efficiently prevented by dextran sulfate (DS) at pH 7.8 [15]. DS binding was assumed to transform the protein into polyanionic species, and the complexes may have provided a sufficient level of electrostatic repulsion at pH 7.8 and 75 °C to prevent the aggregation of the protein from proceeding [15]. Much was the same in the case of β-Lactoglobulin aggregation [16]. It was suggested that DS perturbed the water structure surrounding the protein and stabilize its native form. As far as refolding process is concerned, heparin has been introduced as a possible artificial chaperone to aid protein refolding [17,39].

In the present work, our experiments also identified that DS effectively prevented heat induced aggregation of net negatively charged BSA. In addition, other diverse effects of DS on proteins were observed. To clarify these phenomena and to get new insights into the nature of GAGs–protein interaction, understanding the right mechanisms of the suppression of the aggregation of the proteins are requested. Therefore, using BSA and DS as a model system, we investigated the mechanism by which DS prevents thermally induced aggregation of BSA.

2. Materials and methods

2.1. Sample preparation

BSA and DS were purchased from Sigma (St. Louis, MO). DS employed in this study had a molecular weight of 8.0±0.1 kDa and contained ca. 30 sulfated disaccharides units. BSA solutions (1 mg/ml) with or without DS were prepared in 0.1 M phosphate buffer, and filtered through 0.22 μm filters, as described previously [20,21]. To measure the concentration of BSA, absorption intensity was measured at 279 nm. CD and DLS measurements were performed using different aliquots of the same freshly prepared sample. Samples were degassed in order to prevent the bubble formation in the course of measurements. All kinetic measurements were scrupulously checked against bubble formation before and after each measurement. Partially unfolded BSA was obtained by heating 0.1% (w/w) solution of BSA at 67 °C for 25 min and rapidly cooling the solution in an ice bath as described elsewhere [20,21].

2.2. Heat-induced protein aggregation assay

The heat-induced aggregation of BSA was measured by monitoring the turbidity at 360 nm as a function of pH [39]. BSA was diluted to a final concentration of 1 mg/ml in 0.1 M phosphate buffers with different pH. The BSA solutions were incubated at 73 °C in the presence or absence of 0.1 mM DS, and the apparent absorbance was monitored in a Beckman spectrophotometer (Beckman Coulter, Inc, USA).

2.3. Dynamic light scattering (DLS)

Scattering intensity measurements were performed on an Otsuka ELS-8000 (Osaka, Japan), at a fixed 90° scattering angle with a 10 mW He–Ne laser (wavelength, λ=632.8 nm) [19]. The reported step-wise temperature changes from 25 °C to higher temperatures were obtained by transferring the specimen rapidly from room temperature to the thermostatted sample cell of the instrument. The same samples (1 mg/ml BSA in 0.1 M phosphate buffer) were heated at a constant rate of 0.05 °C/min from 30 °C to 80–90 °C.

2.4. Isothermal titration calorimetry (ITC)

The heat flow resulting from the binding of the DS to BSA was measured using Microcal VP-ITC calorimeter (Microcal, Northampton, MA) with a reaction cell volume of 1.4437 mL [36]. Two types of titrations were performed. In the first measurement, the calorimeter cell contained the BSA solution at a low concentration (C^0_{BSA}=20 μM) was titrated with V_{inj}=10 μL aliquots of concentrated DS solution (C^0_{DS}=500 μM, in 0.1 M phosphate buffer) in every 2.5 min at 25 °C. In the other experiments, the order of solutions was changed, and the calorimeter cell containing the DS at low concentration (C^0_{DS}=25 μM) was injected with BSA solution (400 μM, in 0.1 M phosphate buffer) in every 2.5 min at 25 °C. Integration of the titration peaks yielded the heats of reaction ΔH_{dex} as a function of the molar ratio of DS/BSA. Control titrations were performed to obtain the heat of dilution by injecting the DS solution or the BSA solution into the buffer without counterpart BSA or DS, respectively. The corresponding heat of dilution was subtracted from the heat measured for the binding reaction. For the DS, the heat of dilution was in the range of − 1.0 ∼ − 0.5 μcal, and for the concentrated BSA solutions, the heat of dilution was about − 0.1 μcal. To remove air bubbles, all solutions were degassed prior to use (140 mbar, 8 min). The data were acquired by the software developed by Microcal. The heat measured for the first injection was usually a few percent lower due to the diffusive mixing in the syringe tip during the baseline acquisition. To minimize the impact of this, a minimal volume of 1 μL was always used for the first injection, and the accompanying heat was not used for further analysis [22].

2.5. Circular dichroism (CD)

CD spectra of BSA were recorded using a J-715 Jasco spectropolarimeter (Jasco Co., Tokyo) equipped with a temperature control system in a continuous mode in the wavelength range 200–250 nm (far-UV) and 250–320 nm (near-UV), with a cell having a path lengths of 0.1 cm and 1 cm, and the sample concentration of 0.1 mg/ml and 1 mg/ml, respectively. The spectra were averaged with five scans, corrected with the appropriate buffer blanks and converted to mean residue elasticity (deg cm^2/dmol). All CD measurements were carried out with a bandwidth of 0.5 nm, a response time of 1 s, and a scan speed of 10 nm/min at 25 °C. The protein samples for CD measurements were prepared in 0.1 M sodium phosphate buffer (pH 5.1, 5.9, 6.2, 7.5). Thermal denaturation experiments were performed using a heating rate of 0.5 °C/min and a response time of 1 s. The thermal scan data were collected at every 0.1 °C from 30 to 90 °C in 1 cm path length cuvettes with protein concentrations of 0.1 mg/ml BSA for wavelength of 208 nm and 1 mg/ml BSA for 268 nm.

3. Results

3.1. The prevention of BSA aggregation by DS depends upon pH

Due to the pH dependency of the BSA aggregation [18], we thus investigated the DS effect on the BSA aggregation at several pH values. Initially, the heat-induced BSA aggregation was quantitatively assessed at three different pH values by

measuring the turbidity at 73 °C as a function of incubation time. A pH value of 6.2 was selected since the aggregation occurs through the formation of intermediate at this pH [19–21], and two other pH values above and below this point to see the differences. As shown in Fig. 1, there was no increase in turbidity at any pH value except pH 5.1, where large extent of aggregates formed quickly. However, in the presence of 0.1 mM DS, detectable aggregation was totally prevented at pH 5.1. Although the temperature (73 °C) used in here was well above the 69 °C, the highest temperature used in studying the oligomerization [19], any significant turbidity was not observed at pH 6.2 and pH 7.5. Therefore, the light scattering signal with thermal scan was measured to obtain more detailed ideas of BSA aggregation along with the effect of DS.

Light scattering intensity of the BSA solution was scanned in the course of temperature increase (Fig. 2). An exponential increase in the scattered light intensity was observed approximately above 70 °C at pH 7.5, and the same profile was monitored in the presence of 0.1 mM DS (Fig. 2C). At pH 6.2, scattering intensity began to increase even at lower temperature. At this pH, scattering intensity profile after 67 °C (arrow point in Fig. 2B) was very different in the presence of DS. Diverge of scattering intensity was monitored in the presence of DS above 67 °C, and the DS seemed to prevent the aggregation to some extent at higher temperature. At pH 5.1, scattering intensity sharply increased at 58 °C in the absence of DS (Fig. 2A). The experimental data above 60 °C in the absence of DS is not shown here, because the aggregates formed at this pH were clearly observed at the bottom of the tube. In the presence of DS at pH 5.1, the scattering intensity slightly increased much earlier, but the slope was much lower above ca. 60 °C. In this case, coagulation did not occur within the applied temperature ranges. These results suggested that the prevention of BSA aggregation by DS is dependent upon the pH of the solution.

3.2. DS binds to BSA at pH 5.1 by electrostatic interaction

The results of DLS analysis above suggested that the interaction between DS and BSA is dependent on pH. To investigate the interaction between DS and BSA as a function of pH, ITC analysis was performed (Fig. 3). At pH 5.1, ΔH^0_{dex} initially exhibited a constant large exothermic heat of − 15.5 kcal/mole and then drop sharply to the heat of dilution $\Delta H^{fin}_{dex} \approx -0.01$ kcal/mol. The midpoint of the transition was found at a DS/BSA molar ratio of 0.91±0.01 based on the molecular weights of DS (~8 kDa) and BSA (~67 kDa). The points of the heat of titration were fit to a sigmoidal curve (Fig. 3B) giving the reaction enthalpy at 25 °C as $\Delta H_{dex} = -16.3 \pm 0.2$ kcal/mol of DS and the binding constant of $K_0 = (1.9 \pm 0.2) \times 10^6$ M^{-1}. Gibbs energy change ($\Delta G_{dex} = -8.6 \pm 0.2$ kcal/mol) and entropy change ($\Delta S_{dex} = -7.7 \pm 0.2$ kcal/mol K) were calculated from the value of K_0 and ΔH_{dex} ($\Delta G_{dex} = RT\ln K_0 = \Delta H_{dex} - T\Delta S_{dex}$). The complex formation is mostly driven by a large

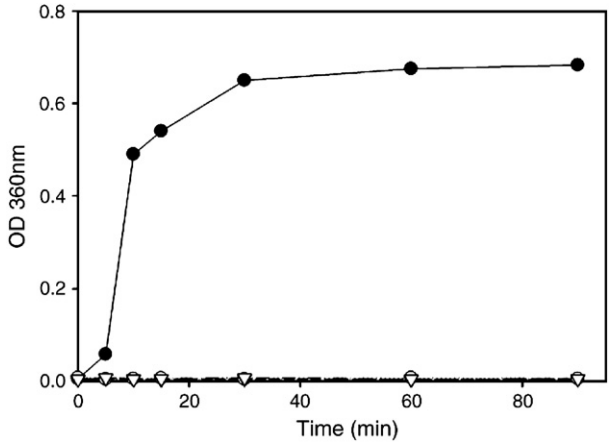

Fig. 1. Heat-induced aggregation of BSA at pH 5.1 (closed circle), pH 6.2 (open circle), pH 7.5 (closed triangle), and pH 5.1 with 0.1 mM DS (open triangle).

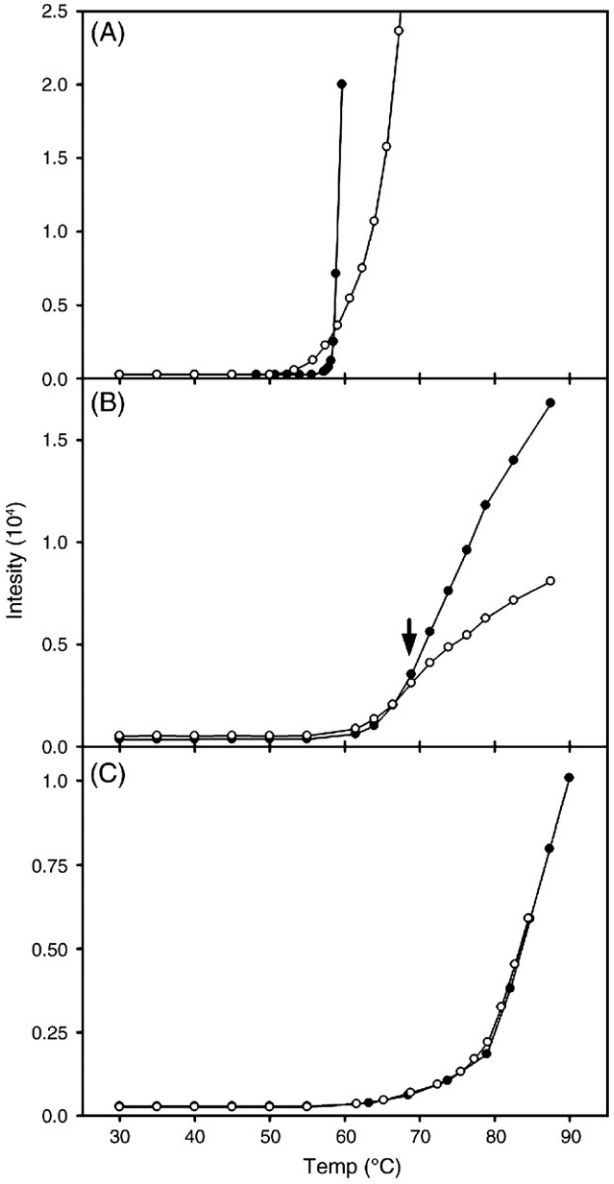

Fig. 2. DLS measurement in the course of temperature scan at pH 5.1 (A), pH 6.2 (B), and pH 7.5 (C). Closed and open circles indicate DLS measurement in the absence of DS and in the presence of 0.1 mM DS, respectively. The arrow indicates that diverge of scattering intensity was monitored in the presence of DS above 67 °C.

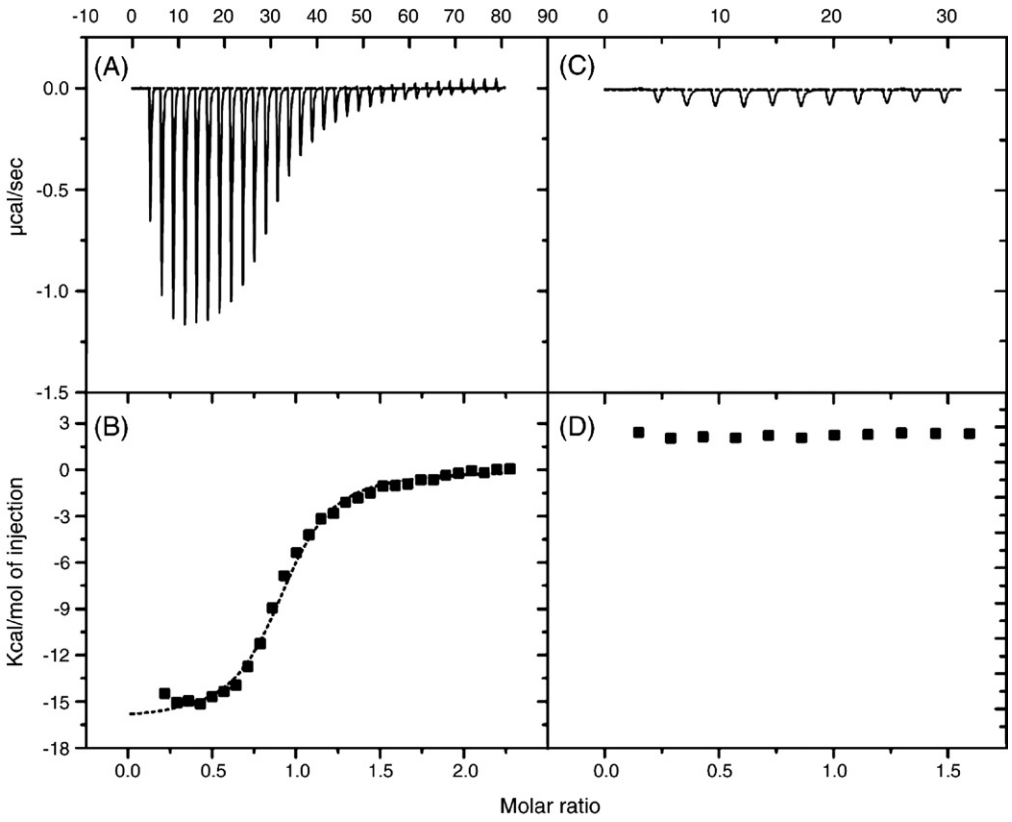

Fig. 3. ITC data for the titration of BSA solution with a concentrated DS solution at pH 5.1 (A, B) and pH 6.2 (C, D). The top panels (A, C) show the raw data after baseline correction. The bottom panels (B, D) show the integrated heat of reaction (solid square) and the best-fit curve (solid line) to a 1:1 binding model.

exothermic enthalpy change [22]. At pH 5.9, the heat flow was significantly decreased and the thermodynamic parameters for binding were much smaller than at pH 5.1 (Table 1). At pH 6.2, 6.7, and 7.5, the dilution heat of DS was only observed as shown in Fig. 3C, and the amount of the heat induced by the binding was too small to be measured. This suggested that the binding between DS and BSA did not occur above pH 6.2.

In Fig. 3A, the heat flow slightly increased at first four injections, implying that another low affinity binding site exists at pH 5.1. To clarify this point, a reverse titration was carried out (Fig. 4). Above pH 5.1, the result didn't show the increase at the first few injections, which is similar to that with dextran-into-BSA titration (data not shown). However, two possible binding sites were detected at pH 5.1. The minimum in the titration curve was reached at DS/BSA ratio ≈2.0, and further addition of BSA led to approximately 1:1 complex. The binding of the first DS molecule was more exothermic than the second.

To find out whether the interaction between BSA and DS depends on electrostatic interaction or hydrophobic interaction, another ITC study was performed as a function of temperature at pH 5.1. The slope of the straight line in Fig. 5 yielded the positive molar heat capacity of $\Delta C_p^0 = 931$ cal/mol·K. This result was in agreement with the characteristic signature of the ionization/charge neutralization reactions, comparing to the hydrophobic reactions with a negative heat capacity [36]. Charge neutralization is accompanied by a positive ΔC_p^0 and may proceed even if ΔH^0 is substantially endothermic because of the positive ΔS^0. Table 2 strongly suggested that the interaction between BSA and DS was accompanied by considerable increase in entropy, indicating that the electrostatic interaction plays a crucial role in BSA–DS binding. While BSA can interact with DS by electrostatic interaction at pH 5.1, BSA lost its electrostatic affinity to DS as pH increased, and the binding did not occur approximately above pH 5.9.

3.3. The strong binding of DS does not stabilize the native state of BSA, rather facilitated denaturation of BSA

A complex formation of DS with BSA could induce conformational changes in the protein structure, and BSA might be stabilized against thermal stress. Recently, several reports indicated that sulfated GAG–protein interaction could induce conformational change of proteins [14,23–25] and in some cases stabilized them. Therefore, to elucidate the structural details of BSA–DS interactions, we investigated the conformation of BSA in the presence of DS using CD spectrometry [49,50]. CD spectra of BSA solutions at various pH in the far-

Table 1
Thermodynamic parameters for binding of dextran sulfate (DS) to BSA as a function of pH

pH	BS [a]	K_0 $M^{-1} \times 10^6$	ΔH_{dex} (kcal/mol DS)	ΔG_{dex} (kcal/mol DS)	$T\Delta S_{dex}$ (kcal/mol DS)
5.1	0.91±0.01	1.9±0.2	−16.3±0.2	−8.6±0.2	−7.7±0.2
5.9	0.33±0.02	1.6±0.1	−11.5±0.2	−7.1±0.2	−4.4±0.2

[a] BS indicates the number of binding sites of DS to BSA.

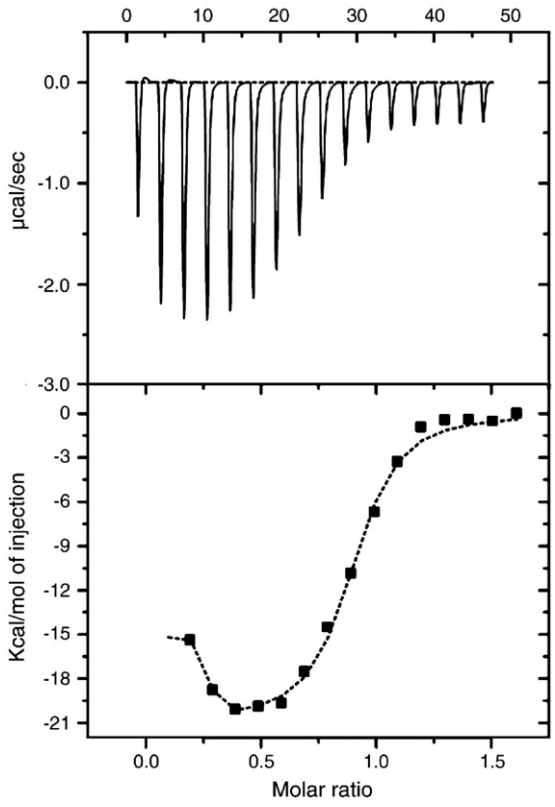

Fig. 4. Titration of DS solution with concentrated BSA solution at pH 5.1. The top panel shows the raw data after baseline correction. The bottom panel shows integrated heat of reaction (solid square) and the best-fit curve (solid line) to a 1:2 binding model.

and near-UV ranges were observed. Observing the two peaks at 208 nm and 222 nm reflecting the dominant contribution of α-helical elements [19,37], the α-structure content showed little difference at different pH (data not shown). Even at pH 5.1, α-helix contents did not change in the presence of 0.1 mM DS. This result suggested that the interaction of DS with BSA did not change the α-helix contents of BSA. Signals were measured in near-UV range to observe the transitions of the aromatic residues and disulphide bonds of BSA [19]. The results revealed that no conformational change did occur neither at different pH nor in the presence of DS (data not shown). In summary, the CD analysis results indicated that the DS binding to BSA did not induce the changes in secondary and tertiary structure of BSA at room temperature.

Near-UV CD spectra were used to monitor the effect of DS binding on the thermal unfolding of BSA as a function of pH (Fig. 6). Although the exact melting temperature could not be determined due to the fluctuations in the signals at higher temperature, it was possible to compare the differences with DS during the thermal scanning. At pH 7.5, DS did not induce any change in the tertiary structure profile of BSA, and the apparent melting temperatures ($T_{m,apparent}$) were quite similar; 71.3 ± 1 °C in the absence of DS and 70.1 ± 1 °C in the presence of 0.1 mM DS. However, as the pH became lower, the $T_{m,apparent}$ values significantly decreased in the presence of DS. For example, at pH 5.1, $T_{m,apparent}$ value shifted to a much lower temperature, 62.9 ± 1 °C and the negative ellipticity had significantly smaller value than that in the absence of DS. These results suggested that the interaction between DS and BSA facilitated the heat induced opening and structural changes of BSA rather than stabilizing its native state.

3.4. DS was able to bind to the partially unfolded BSA at pH 6.2

Electrostatic repulsion induced by the formation of BSA–DS complexes has often been suggested as a feasible mechanism of suppressing protein aggregation. However, ITC results suggest that DS does not bind to the native BSA above pH 5.9, which means other mechanisms must present to explain the suppression of BSA aggregation in the presence of DS at pH 6.2 (Fig. 2). At pH 6.2, the light scattering intensity profiles with and without DS were very similar up to 67 °C. However, diverge of the light scattering intensity was monitored in the presence of DS above 67 °C (arrow point indicated in Fig. 2), while no electrostatic interaction was expected according to the ITC results at this pH (Fig. 3). This contradictory results and the fact that significant change of the tertiary structure of BSA occur around 67 °C [19–21] suggest a possible mechanism of the complex formation of DS-partially unfolded BSA at pH 6.2. To prove this hypothesis, ITC analysis was applied to investigate the interaction between DS and partially unfolded BSA. Partially unfolded BSA was obtained by heating 0.1% (w/w) solution of BSA at 67 °C for 25 min and rapidly cooling the solution in an ice bath as described elsewhere [20,21]. As shown in Fig. 7, DS bound to the partially unfolded BSA at pH 6.2 (Fig. 7A), but not at pH 6.7 and 7.5 (data not shown). On the other hand, control experiments indicated that there was no interaction between DS and native BSA even at pH 6.2 (Fig. 7C). This result suggests that DS can bind to the partially unfolded BSA at pH 6.2 at which native BSA does not interact with DS.

4. Discussion

The heat induced aggregation mechanism of BSA at concentrations of far below 0.1% (w/w) has been extensively

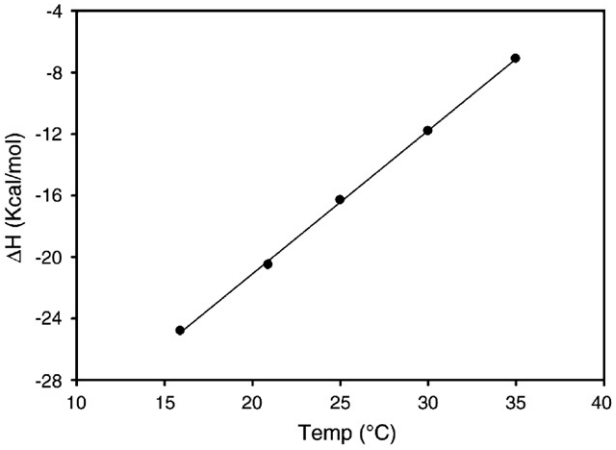

Fig. 5. Temperature dependence of the reaction enthalpy, ΔH^0 for DS binding to BSA. Solid circle and solid line show the experimental results and linear regression, respectively.

Table 2
Thermodynamic parameters for binding of dextran sulfate (DS) to BSA as a function of temperature

Temperature (°C)	BS [a]	K_0 $M^{-1} \times 10^6$	ΔH_{dex} (kcal/mol DS)	ΔG_{dex} (kcal/mol DS)	$T\Delta S_{dex}$ (kcal/mol DS)
15.9	0.91	2.93	−24.8	−8.6	−16.3
20.9	0.88±0.01	2.3±0.2	−20.5±0.2	−8.6±0.2	−11.9±0.2
25	0.91±0.01	1.9±0.2	−16.3±0.2	−8.6±0.2	−7.7±0.2
30	0.87±0.01	1.7±0.2	−11.8±0.1	−8.6±0.1	−3.1±0.1
35	0.87	1.22	−7.1	−8.5	1.5

[a] BS indicates the number of binding sites of DS to BSA.

studied. The mechanism comprised of two distinctive processes: protein unfolding/misfolding and oligomerization followed by aggregation [18–21,40,41,43]. It has been generally accepted that the oligomerization is facilitated by the formation of denatured protein. Considering the general aggregation mechanism mentioned above, we expected in largely two ways DS could suppress the aggregation of BSA. One is to prevent the formation of denatured BSA by stabilizing native BSA and the other is to prevent the oligomerization. In this study, we showed that DS strongly bound to BSA at pH 5.1 using ITC analysis (Fig. 3(A)). Similar to Anthithrombin III [14,44,45], a conformational change of BSA induced by the complex formation of BSA–DS could be more favorable to resist thermal stress [14,42,44,45]. However, the addition of DS did not lead to neither tertiary nor secondary structural changes at pH 5.1 (data not shown). On the contrary, the near-UV CD analysis at 268 nm showed the increased exposure of aromatic residues to the solvent during the thermal scanning in the presence of DS (Fig. 6 (A)) [19], which means the unfolding of BSA is rather facilitated by the addition of DS at pH 5.1. Therefore, the DS could suppress the aggregation by preventing the oligomerization rather than by supporting more stable structures at pH 5.1.

Recent studies have identified three major properties of protein that determine the degree of conversion of the partially or totally unfolded state into aggregates; hydrophobicity, high propensity to convert from α-helical to β-sheet structure, and a low net charge [26–33]. Proteins "natively unfolded" under physiological conditions generally have a lower content of hydrophobic residues, and exhibit higher total net charge than its corresponding folded globular proteins [34]. This appears to be a surviving strategy for the non-globular proteins to avoid aggregation and to remain soluble in the crowded environment of cell cytoplasm [35]. Previous studies have shown that BSA can bind to heparin and other polyelectrolytes at pH values above pI of BSA (pI ≈4.9). It indicated the existence of a local protein domain, which makes binding to a strong polyanion such as heparin possible at certain conditions [46,47,51]. Strong effects of pH and ionic strength on the amount of BSA bounds also indicate that the interaction is mainly due to coulombic force between GAGs and BSA [47,51]. These results are well matched with our ITC result at pH 5.1, where DS strongly bind to BSA with dominant electrostatic interaction (Fig. 5). Similar to heparin, DS may bind to the positively charged local protein domain of BSA [47,48,51]. In this manner, the DS may shield the positively charged domain of BSA. Moreover, one DS molecule bound to one BSA molecule tends to increase the net negative charge of the DS–BSA complex approximately up to 27, since DS of 8000 Da has 27 glycosyl residues per one molecule. Once the net charge of a protein becomes higher, interactions between the proteins could be hindered by an overall effect of electrostatic repulsion. Thus, an increase in the

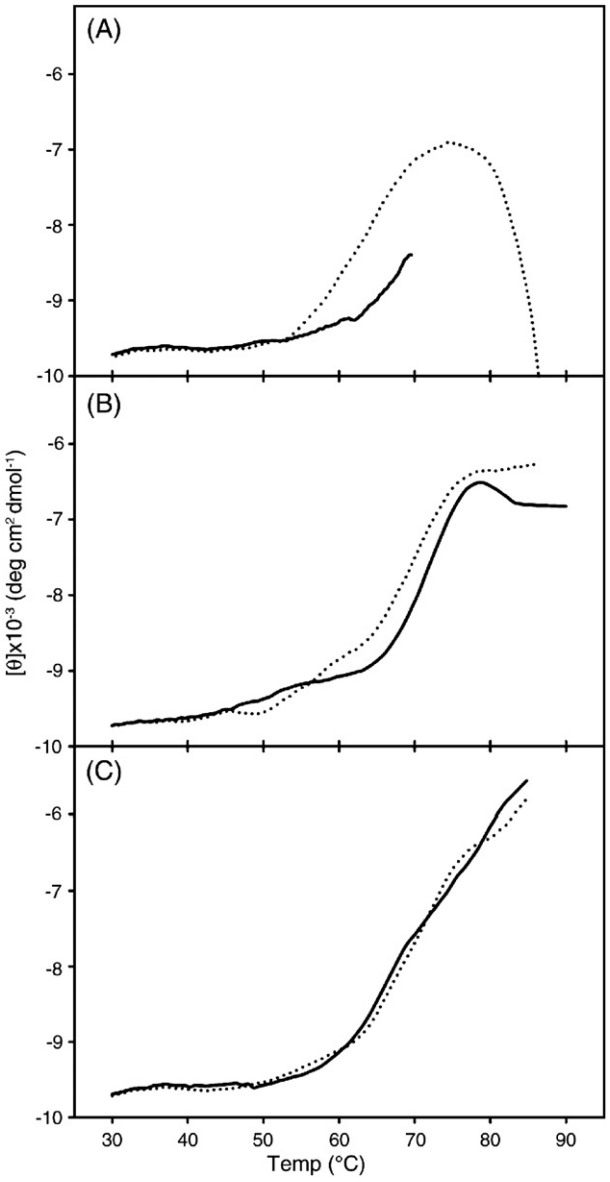

Fig. 6. Effect of DS on the thermal denaturation of BSA in the absence of DS (solid line) and in the presence of 0.1 mM DS (dotted line). Denaturation was monitored by the changes in ellipticity in the near-UV CD at 268 nm; (A) at pH 5.1, (B) at pH 6.2, (C) at pH 7.5.

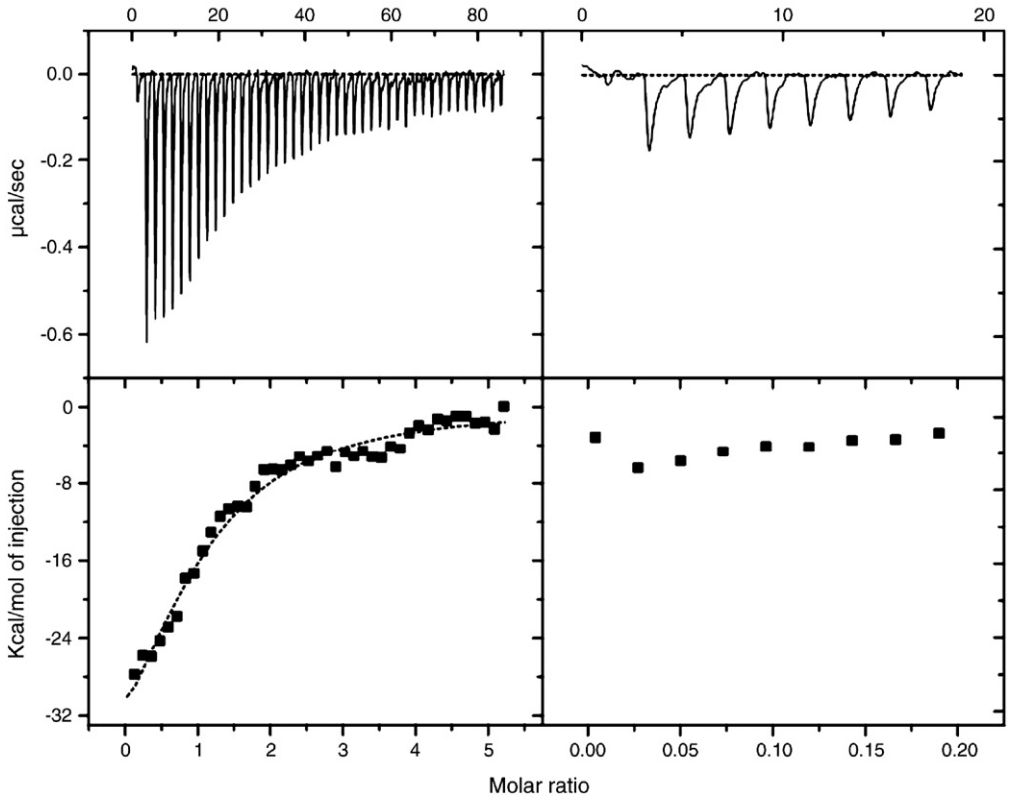

Fig. 7. Interaction between intermediate BSA and DS (A, B) and between native BSA and dextran sulfate (C, D) at 25 °C in 100 mM phosphate buffer and pH 6.2. The bottom panels show integrated heats (solid square) and the best-fit curve (solid line) by using 1:1 binding models. Left panels (A, B) show that 200 μM DS was titrated into 30 μM intermediate BSA, with the injection volume of 5 μL, and the right panels (C, D) show that 200 μM DS was titrated into 30 μM native BSA, with the injection volume of 5 μL.

net charge of BSA due to DS binding could lead to an enhancement in the extent of such repulsions, contributing to the suppression of the further oligomerization or aggregation.

The electrorepulsion followed by the complex formation between BSA and DS could also explain the effect of DS on the suppression of the aggregation at pH 6.2. DS did not bind to native BSA at pH 6.2 according to our ITC results (Fig. 3). Even if there is a possibility that the heat released by DS–BSA binding might be too small to be detected by ITC, the weak interaction would be hard to be maintained at high temperature. Since the binding interaction between BSA and DS is mainly exothermic, it should be much weaker at high temperature (Table 2). However, the additional ITC analysis showed that DS can bind to the partially unfolded BSA at pH 6.2 (Fig. 7). It probably means the conformational changes of partially unfolded BSA would make the protein more susceptible to bind to DS. Also, by the fact that the light scattering intensity profile was abruptly differentiated around 67 °C in the presence of DS (Fig. 2(B)), we suggest that once the DS-unfolded BSA complex is formed, then it can resist further aggregation probably by electrorepulsion between complexes.

The results presented here illustrate the mechanism by which DS suppresses protein aggregation. Three interesting points were elaborated. First of all, DS–protein complex formation is a prerequisite for this role. Secondly, strong electrostatic interaction between BSA and DS can rather facilitate denaturation of protein. This result limits the usage of DS as a stabilizer and aggregation inhibitor proposed by other studies. Lastly, DS can bind to the partially unfolded state of protein generated by heat stress at pH 6.2. To the best of our knowledge, this is the first report showing that using ITC analysis, GAGs can clearly form a complex with the partially unfolded protein despite the presence of electrostatic repulsion, and thereby possibly suppress the aggregation of the protein. It was suggested that heparin interacts with a normally transient soluble oligomers, and then facilitates fibrillation [8]. Similarly, it is likely that the transition of α-synuclein from an unstructured state to the one containing substantial β-sheet creates a favorable conformation for the binding with GAGs, resulting in a highly localized α-synuclein concentration that favors fibrillation. However, in the case of DS, DS-unfolded protein complex rather hindered the local increase in protein concentration probably by electrorepulsion between complexes. The distinctive difference between the two phenomena might originate from the structural difference in the unfolded state of proteins and the nature of the binding between soluble proteins and DS.

Acknowledgments

This research was partially supported by Nano Bioelctronics and System Research Center supported by KOSEF, Brain Korea 21 program of Korea and National R and D Program Grant of

the Ministry of Science and Technology (M10417060004-04N1706-00410).

References

[1] M. Goedert, R. Jakes, M.G. Spillantini, M. Hasegawa, M.J. Smith, R.A. Crowther, Assembly of microtubule-associated protein tau into Alzheimer-like filaments induced by sulphated glycosaminoglycans, Nature 383 (1996) 550–553.

[2] M. Necula, C.N. Chirita, J. Kuret, Rapid anionic micelle-mediated alpha-synuclein fibrillization in vitro, J. Biol. Chem. 278 (2003) 46674–46680.

[3] J.D. Sipe, Amyloidosis, Annu. Rev. Biochem. 61 (1992) 947–975.

[4] P.E. Fraser, J.T. Nguyen, D.T. Chin, D.A. Kirschner, Effects of sulfate ions on Alzheimer beta/A4 peptide assemblies: implications for amyloid fibril–proteoglycan interactions, J. Neurochem. 59 (1992) 1531–1540.

[5] R. Gupta-Bansal, R.C.A. Frederickson, K.R. Brunden, Proteoglycan-mediated inhibition of A beta proteolysis. A potential cause of senile plaque accumulation, J. Biol. Chem. 270 (1995) 18666–18671.

[6] L.M. Shaffer, M.D. Dority, R. Gupta-Bansal, R.C.A. Frederickson, S.G. Younkin, K.R. Brunden, Amyloid beta protein (A beta) removal by neuroglial cells in culture, Neurobiol. Aging 16 (1995) 737–745.

[7] G.M. Castillo, C. Ngo, J. Cummings, T.N. Wight, A.D. Snow, Perlecan binds to the beta-amyloid proteins (A beta) of Alzheimer's disease, accelerates A beta fibril formation, and maintains A beta fibril stability, J. Neurochem. 69 (1997) 2452–2465.

[8] A.D. Cardin, H.J. Weintraub, Molecular modeling of protein–glycosaminoglycan interactions, Arteriosclerosis 9 (1989) 21–32.

[9] R. Jakes, M.G. Spillantini, M. Goedert, Identification of two distinct synucleins from human brain, FEBS Lett. 345 (1994) 27–32.

[10] J.C. Rochet, K.A. Conway, P.T. Lansbury Jr., Inhibition of fibrillization and accumulation of prefibrillar oligomers in mixtures of human and mouse alpha-synuclein, Biochemistry 39 (2000) 10619–10626.

[11] H.K. Paudel, W. Li, Heparin-induced conformational change in microtubule-associated protein Tau as detected by chemical cross-linking and phosphopeptide mapping, J. Biol. Chem. 274 (1999) 8029–8038.

[12] J. McLaurin, T. Franklin, X. Zhang, J. Deng, P.E. Fraser, Interactions of Alzheimer amyloid-beta peptides with glycosaminoglycans effects on fibril nucleation and growth, Eur. J. Biochem. 266 (1999) 1101–1110.

[13] J.A. Cohlberg, J. Li, V.N. Uversky, A.L. Fink, Heparin and other glycosaminoglycans stimulate the formation of amyloid fibrils from alpha-synuclein in vitro, Biochemistry 41 (2002) 1502–1511.

[14] T.F. Busby, D.H. Atha, K.C. Ingham, Thermal denaturation of antithrombin III. Stabilization by heparin and lyotropic anions, J. Biol. Chem. 256 (1981) 12140–12147.

[15] A.M. Tsai, J.H. van Zanten, M.J. Betenbaugh II, Electrostatic effect in the aggregation of heat-denatured RNase A and implications for protein additive design, Biotechnol. Bioeng. 59 (1998) 281–285.

[16] G. Zhang, E.A. Foegeding, C.C. Hardin, Effect of sulfated polysaccharides on heat-induced structural changes in beta-lactoglobulin, J. Agric. Food Chem. 52 (2004) 3975–3981.

[17] F. Meng, Y. Park, H. Zhou, Role of proline, glycerol, and heparin as protein folding aids during refolding of rabbit muscle creatine kinase, Int. J. Biochem. Cell Biol. 33 (2001) 701–709.

[18] V. Militello, C. Casarino, A. Emanuele, A. Giostra, F. Pullara, M. Leone, Aggregation kinetics of bovine serum albumin studied by FTIR spectroscopy and light scattering, Biophys. Chem. 107 (2004) 175–187.

[19] S.M. Vaiana, A. Emanuele, M.B. Palma-Vittorelli, M.U. Palma, Irreversible formation of intermediate BSA oligomers requires and induces conformational changes, Proteins 55 (2004) 1053–1062.

[20] P.L. San Biagio, V. Martorana, A. Emanuele, S.M. Vaiana, M. Manno, D. Bulone, M.B. Palma-Vittorelli, M.U. Palma, Interacting processes in protein coagulation, Proteins 37 (1999) 116–120.

[21] P.L. San Biagio, D. Bulone, A. Emanuele, M.U. Palma, Self-assembly of biopolymeric structures below the threshold of random cross-link percolation, Biophys. J. 70 (1996) 494–499.

[22] T.G. Anderson, A. Tan, P. Ganz, J. Seelig, Calorimetric measurement of phospholipid interaction with methyl-beta-cyclodextrin, Biochemistry 43 (2004) 2251–2261.

[23] H.K. Paudel, W. Li, Heparin-induced conformational change in microtubule-associated protein Tau as detected by chemical cross-linking and phosphopeptide mapping, J. Biol. Chem. 274 (1999) 8029–8038.

[24] M.A. Jairajpuri, A. Lu, U. Desai, S.T. Olson, I. Bjork, S.C. Bock, Antithrombin III phenylalanines 122 and 121 contribute to its high affinity for heparin and its conformational activation, J. Biol. Chem. 278 (2003) 15941–15950.

[25] Y.H. Lin, W.N. Huang, S.C. Lee, W.G. Wu, Heparin reduces the α-helical content of cobra basic phospholipase A_2 and promotes its complex formation, Int. J. Biol. Macromol. 27 (2000) 171–176.

[26] F. Chiti, M. Calamai, N. Taddei, M. Stefani, G. Ramponi, C.M. Dobson, Studies of the aggregation of mutant proteins in vitro provide insights into the genetics of amyloid diseases, Proc. Natl. Acad. Sci. U. S. A. 99 (2002) 16419–16426.

[27] C. Hilbich, B. Kisters-Woike, J. Reed, C.L. Masters, K. Beyreuther, Substitutions of hydrophobic amino acids reduce the amyloidogenicity of Alzheimer's disease beta A4 peptides, J. Mol. Biol. 228 (1992) 460–473.

[28] D.E. Otzen, O. Kristensen, M. Oliveberg, Designed protein tetramer zipped together with a hydrophobic Alzheimer homology: a structural clue to amyloid assembly, Proc. Natl. Acad. Sci. U. S. A. 97 (2000) 9907–9912.

[29] L. Tjernberg, W. Hosia, N. Bark, J. Thyberg, J. Johansson, Charge attraction and beta propensity are necessary for amyloid fibril formation from tetrapeptides, J. Biol. Chem. 277 (2002) 43243–43246.

[30] T. Konno, Amyloid-induced aggregation and precipitation of soluble proteins: an electrostatic contribution of the Alzheimer's beta(25–35) amyloid fibril, Biochemistry 40 (2001) 2148–2154.

[31] M. Lopez De La Paz, K. Goldie, J. Zurdo, E. Lacroix, C.M. Dobson, A. Hoenger, L. Serrano, De novo designed peptide-based amyloid fibrils, Proc. Natl. Acad. Sci. U. S. A. 99 (2002) 16052–16057.

[32] B. Ciani, E.G. Hutchinson, R.B. Sessions, D.N. Woolfson, A designed system for assessing how sequence affects alpha to beta conformational transitions in proteins, J. Biol. Chem. 277 (2002) 10150–10155.

[33] Y. Kallberg, M. Gustafsson, B. Persson, J. Thyberg, J. Johansson, Prediction of amyloid fibril-forming proteins, J. Biol. Chem. 276 (2001) 12945–12950.

[34] V.N. Uversky, J.R. Gillespie, A.L. Fink, Why are "natively unfolded" proteins unstructured under physiologic conditions? Proteins 41 (2000) 415–427.

[35] M. Calamai, N. Taddei, M. Stefani, G. Ramponi, F. Chiti, Relative influence of hydrophobicity and net charge in the aggregation of two homologous proteins, Biochemistry 42 (2003) 15078–15083.

[36] A. Ziegler, J. Seelig, Interaction of the protein transduction domain of HIV-1 TAT with heparan sulfate: binding mechanism and thermodynamic parameters, Biophys. J. 86 (2004) 254–263.

[37] N. Greenfield, G.D. Fasman, Computed circular dichroism spectra for the evaluation of protein conformation, Biochemistry 8 (1969) 4108–4116.

[38] J.M. Dabora, G. Sanyal, C.R. Middaugh, Effect of polyanions on the refolding of human acidic fibroblast growth factor, J. Biol. Chem. 266 (1991) 23637–23640.

[39] B.M. Eckhardt, J.Q. Oeswein, D.A. Yeung, T.D. Milby, T.A. Bewley, A turbidimetric method to determine visual appearance of protein solutions, J. Pharm. Sci. Technol. 48 (1994) 64–70.

[40] P.L. San Biagio, M.U. Palma, Spinodal lines and Flory–Huggins free-energies for solutions of human hemoglobins HbS and HbA, Biophys. J. 60 (1991) 508–512.

[41] R. Wetzel, M. Becker, H. Billwitz, S. Bohm, B. Ebert, H. Hamann, J. Krumbiegel, G. Lassmann, Temperature behaviour of human serum albumin, Eur. J. Biochem. 104 (1980) 469–478.

[42] U.S. Cho, H.J. Ahn, E.Y. Park, M.S. Dong, K.H. Kim, Influence of ligand binding to human cytochrome P-450 1A2: conformational activation and stabilization by alpha-naphthoflavone, Biochim. Biophys. Acta 1546 (2001) 412–421.

[43] K. Murayama, M. Tomida, Heat-induced secondary structure and conformation change of bovine serum albumin investigated by Fourier transform infrared spectroscopy, Biochemistry 43 (2004) 11526–11532.

[44] B. Nordenman, I. Bjork, Binding of low-affinity and high-affinity heparin

to antithrombin. Ultraviolet difference spectroscopy and circular dichroism studies, Biochemistry 17 (1978) 3339–3344.
[45] S.T. Olson, K.R. Srinivasan, I. Bjork, J.D. Shore, Binding of high affinity heparin to antithrombin III. Stopped flow kinetic studies of the binding interaction, J. Biol. Chem. 256 (1981) 11073–11079.
[46] K.R. Grymonpre, B.A. Staggemeier, P.L. Dubin, K.W. Mattison, Identification by integrated computer modeling and light scattering studies of an electrostatic serum albumin-hyaluronic acid binding site, Biomacromolecules 2 (2001) 422–429.
[47] E. Seyrek, P.L. Dubin, C. Tribet, E.A. Gamble, Ionic strength dependence of protein–polyelectrolyte interactions, Biomacromolecules 4 (2003) 273–282.
[48] J.M. Park, B.B. Muhoberac, P.L. Dubin, J. Xia, Effects of protein charge heterogeneity in protein–polyelectrolyte complexation, Macromolecules 25 (1992) 290–295.
[49] A.A Vyas, J. Pan, H.V. Patel, K.A. Vyas, C. Chiang, Y. Sheu, J. Hwang, W. Wu, Analysis of binding of cobra cardiotoxins to heparin reveals a new β-sheet heparin-binding structural motif, J. Biol. Chem. 272 (1997) 9661–9670.
[50] L.M. Lima, G. de Prat-Gay, Conformational changes and stabilization induced by ligand binding in the DNA-binding domain of the E2 protein from human papillomavirus, J. Biol. Chem. 272 (1997) 19295–19303.
[51] T. Hattori, K. Kimura, E. Seyrek, P.L. Dubin, Binding of bovine serum albumin to heparin determined by turbidimetric titration and frontal analysis continuous capillary electrophoresis, Anal. Biochem. 295 (2001) 158–167.